J. Phase Equilib. Diffus.
DOI 10.1007/s11669-017-0537-8

A Thermodynamic Study of a Constitutional Diagram for Duplex Stainless Steels

Sérgio Duarte Brandi[1] · **Cláudio Geraldo Schön**[1]

Submitted: 15 November 2016 / in revised form: 9 February 2017

Abstract Arc welding involves joining two metal plates by a welding pool, which is kept molten for short periods due to an electric arc. This weld metal has, sometimes, a different composition from the plates, due to a filler metal. Arc welding is a non-equilibrium process. Technological approach, nevertheless, uses empirical tools to predict important features of the joints. In stainless steel welding, the Schaeffler diagram, and other constitutive diagrams, as the WRC 1992 diagram, are used to predict the resultant microstructure in the welded joint. The composition input is calculated by Chromium and Nickel equivalents expressions. Schaeffler diagram is used to evaluate weldability of stainless steels. Some people adapt the W and N alloying elements in Schaeffler diagram to predict the weldability of duplex stainless steels (DSS). Present work shows how these technological tools can be understood as results of phase equilibrium in key isotherms of the Fe-Cr-Ni system, used in all constitutive diagrams. The validity and limitation of the Chromium and Nickel equivalents expressions were discussed based on the effect of up to two alloying components (X_1 = Mo or W and X_2 = N) on the alpha/gamma phase equilibrium, as estimated by calculations in system Fe-Cr-Ni-X_1-X_2 that are typical DSS alloying elements. This allows extending these Chromium and Nickel equivalents expressions based on thermodynamics and to identify vulnerabilities for two important problems in DSS welding: Chromium nitride and sigma phase precipitation. Originally, Schaeffler's diagram does not consider the effect of W and N in the ($\gamma/\alpha + \gamma$) equilibrium field.

Keywords duplex stainless steel · Schaeffler diagram · thermodynamic assessment · weldability

1 Introduction

Constitutional diagrams, such as Schaeffler,[1–3] DeLong[4,5] and WRC-92 diagrams,[6,7] are based in Chromium and Nickel equivalent concepts. Originally in Schaeffler diagram, the phase fields are lines with curvature, suggesting the synergistic effects of stainless steel alloying elements.[8] Latter, these phase fields were replaced in Schaeffler diagram by straight lines, based upon the work of Thomas Jr.[9] These diagrams are depicted in Fig. 1, 2, and 3, respectively.

They have been used to predict weld metal microstructure and weldability of stainless steels in general. The diagram can be applied to a variety of usual arc welding cooling rates,[8] which justify its use in weldability evaluation.[1–7,10] In other words, it is possible to utilize constitutional diagrams to predict the susceptibility to sigma phase and other intermetallic phases precipitation; the amount of ferrite in the weld metal; poor toughness due to ferritic coarse grain in weld metal and HAZ; hydrogen embrittlement in martensitic stainless steels and solidification cracking in austenitic weld metals, that affect the weldability of stainless steels. This prediction is based in the chemical composition of base metal plates, filler metal

This article is an invited paper selected from presentations at TOFA 2016, the Discussion Meeting on Thermodynamics of Alloys, held September 4-9, 2016, in Santos, Brazil, and has been expanded from the original presentation.

✉ Sérgio Duarte Brandi
sebrandi@usp.br

[1] Department of Metallurgical and Materials Engineering, Escola Politécnica da Universidade de São Paulo, São Paulo, São Paulo, Brazil

Published online: 19 April 2017

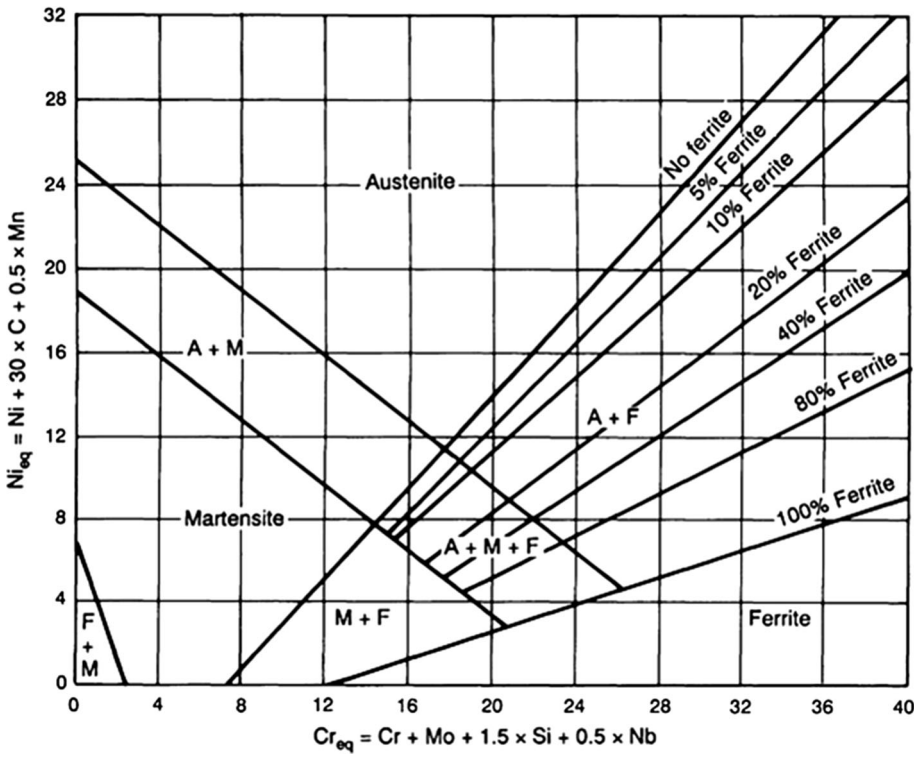

Fig. 1 Schaeffler constitutional diagram[1–3]

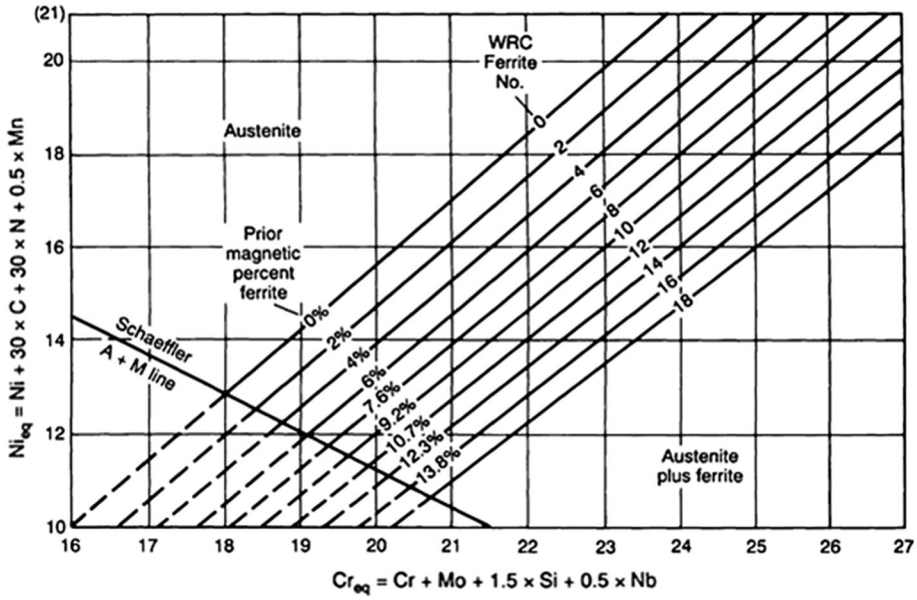

Fig. 2 DeLong constitutional diagram[4,5]

weld metal chemical composition and welding process dilution. Taking all this information into account, a chemical composition point is set in the diagram. Consequently, depending on the weldability field where a welded joint is located, defines the weldability problem. Figure 4 shows Schaeffler diagram with four poor weldability fields. Schaeffler's diagram does not contemplate the effect of W and N in the position, size and shape of these four weldability regions.

2 Thermodynamic Models and Calculation Strategies

The present calculations are made using SGTE Solid Solutions 2.0 (SSOL2) database which is based on the collaborative work of European and Canadian Laboratories (the Scientific Group Thermodata Europe, SGTE). The present work uses a subset of this database corresponding to system Fe-Cr-Ni-N-Mo-W, and, in this system, the

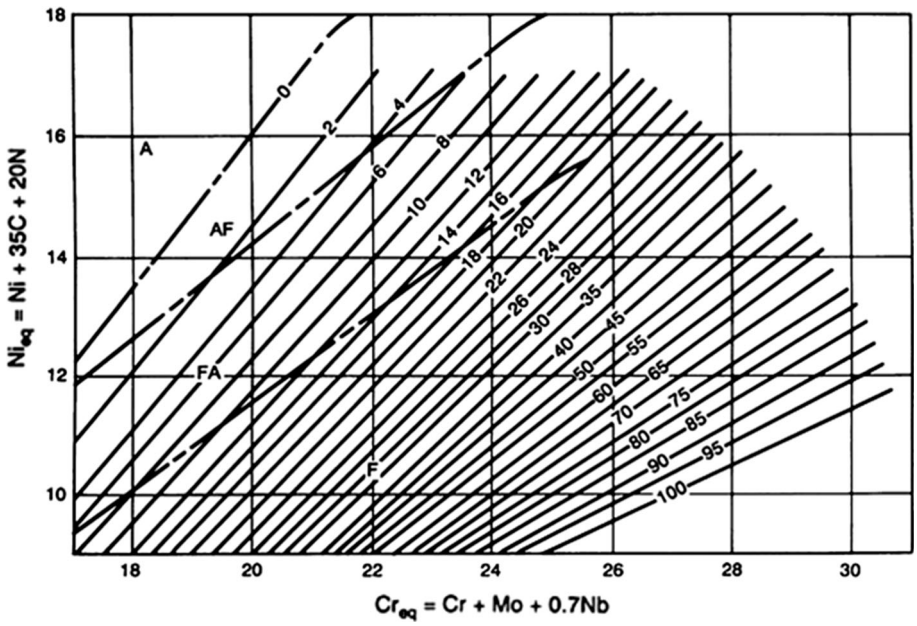

Fig. 3 WRC-92 constitutional diagram[6,7]

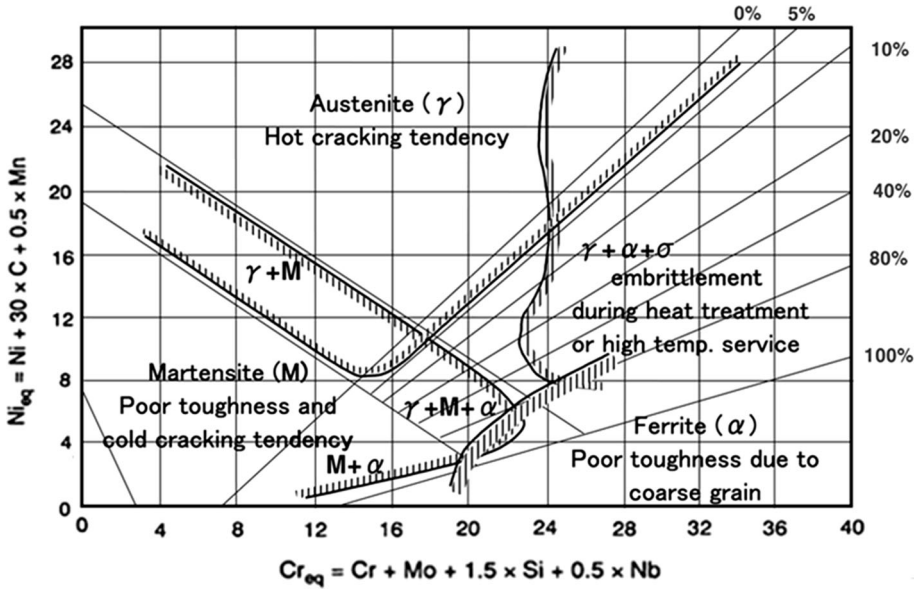

Fig. 4 Schaeffler constitutional diagram adapted to weldability prediction[1–7,10]

phases: liquid, face centered cubic (FCC), body centered cubic (BCC), hexagonal close packed (HCP), σ phase and Laves phase (in the present case the hexagonal C14 version, stable in systems Fe-Mo and Fe-W) were used. Some key compounds in duplex steels are included in this subset, in particular the MN nitride is modeled as a miscibility gap in the FCC phase and the M_2N nitride is modeled as a miscibility gap in the HCP phase.

Part of the data for key systems has been published in accessible works, for example, in Cr-Fe-N.[11] The database relies, however, upon internal reports and unpublished data and may be considered the state-of-art of thermodynamic models for solid solution metallic phases in year 1992 (when it was published). Naturally, other assessment on these systems have been published since then, but, for example, in a recent assessment of system Fe-Cr-C system[12] most of the quoted references are the ones included in the SSOL2 database, so it is considered reliable for the present purposes.

Calculations are divided in three groups:

1. Thermodynamic justification of the basic Schaeffler's diagram, based on isothermal sections in system Fe-Cr-Ni.
2. Thermodynamic justification of the concepts of equivalent Chromium and equivalent Nickel, using a base

composition Fe-25 wt.% Cr-5 wt.% Ni, typical of duplex steels.

3. The discussion of the viability of diagrams for susceptibility to σ and M_2N precipitation.

3 Results and Discussion

3.1 Thermodynamic Justification of Schaeffler's Diagram

Figure 5 shows the isothermal section of the Fe-Cr-Ni system at $T = 1273$ K (1000 °C), in reversing rolling mill technology, typically used in duplex steel production, temperature is kept in the range between 1100 and 1060 °C. The combination of mechanical work and high temperatures create the expectancy that thermodynamic equilibrium is roughly maintained during this process. After this step, the rolled sheet is usually thin and rapid cools so that microstructure is retained, keeping approximately the high temperature equilibrium metastable. The selected temperature seems a good reference to this microstructure. Additional calculations around this temperature show, however, that the phase boundaries are not very sensitive to this parameter. The diagram was plotted in the same scale as the Schaeffler diagram (Fig. 1) and, the besides of the fact that the FCC and BCC boundaries in this diagram are curved lines, the coincidence is remarkable, showing that the basic structure of the phenomenological diagram is validated by thermodynamics. Actually these lines are represented as straight lines, since 1973, but in the original version published by Schaeffler,[1–3] which was determined by experimentation, is even more striking.

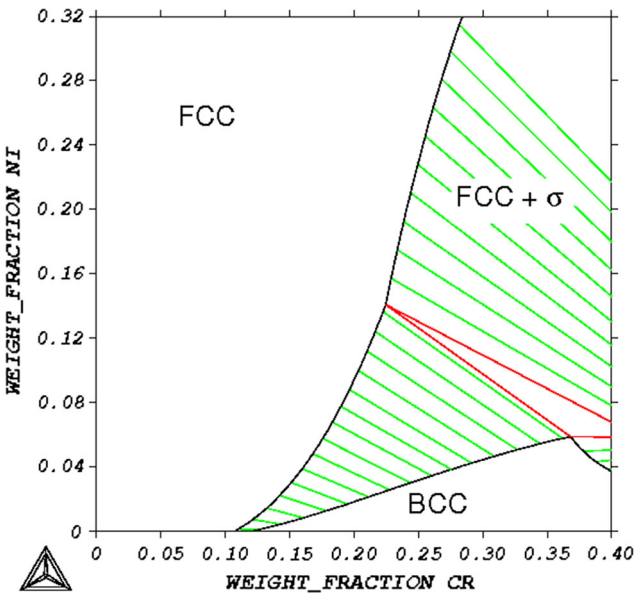

Fig. 5 Isothermal section of system Fe-Cr-Ni at 1273 K (1000 °C) in the same scale of Schaeffler diagram

The Schaeffler diagram, however, is richer in information. It contains fields close to the iron rich corner corresponding to "equilibrium" with martensite. The martensitic transformation in steels requires two minimum conditions to happen: the stability of the austenite phase at high temperatures and the stability of the ferrite phase at low temperatures. The stability of the austenite phase at high temperature in the corresponding fields is consistent with the 1273 K (1000 °C) isotherm (Fig. 1). It is necessary now to show that the ferrite phase (BCC) is also stable in these regions at low temperatures. Figure 6 shows the isothermal section of the Fe-Cr-Ni system at 1073 K (800 °C). Comparing the isothermal sections, we observe that, indeed, close to the iron-rich corner the ferrite phase becomes stable in compositions where the austenite is stable at higher temperatures. Therefore it is possible[1] to exist martensite in these regions, as the Schaeffler diagram predicts.

These results show, therefore, that the basic structure of Schaeffler diagram can be understood because of the thermodynamics of the Fe-Cr-Ni system, as should be expected. This tool, however is, in principle, applicable to multicomponent systems through the concepts of Chromium and Nickel equivalents, and the connection to thermodynamics deserves to be investigated as well.

3.2 Equivalent Chromium and Nickel

Chromium and Nickel equivalents are the names given to certain linear mathematic expressions between the alloying chemical elements composition of the steel. The Chromium equivalent includes alphagenic elements (i.e. those which stabilize the BCC alpha phase, or ferrite), such as molybdenum, silicon and niobium. Nickel equivalent includes gammagenic elements (i.e. those which stabilize the FCC gamma phase, or austenite), like manganese, and carbon. In both formulas, each elemental composition is multiplied by a numeric pre-factor which represents the "power" of each element has to substitute either Chromium or Nickel (in the respective expressions), and stabilizes ferrite or austenite, respectively.

The linear structure of the expressions imply that the different elements act as independent from each other. In other words, the addition of molybdenum neither potentiates nor damps the effect of Chromium, for example. From a thermodynamic perspective, this is a very questionable

[1] Actually the martensitic transformation depends on other factors, the present calculation only shows that the transformation is possible, as a sine qua non condition.

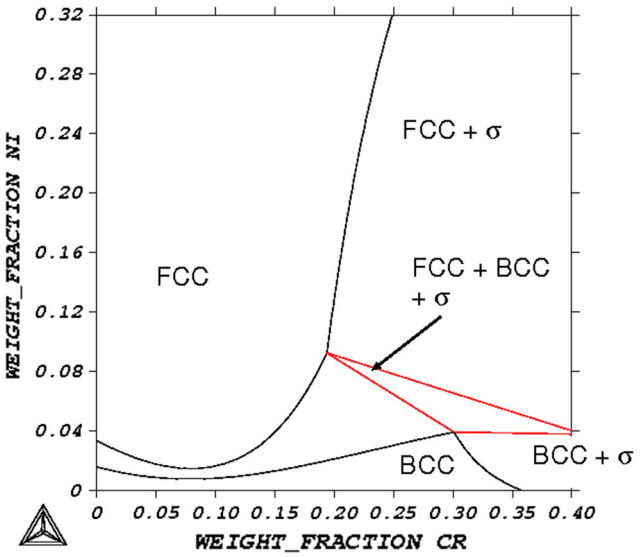

Fig. 6 Isothermal section of system Fe-Cr-Ni at 1073 K (800 °C), showing that ferrite becomes stable in the regions where austenite is stable at higher temperatures, consistent with the possibility of occurrence of martensitic transformation

hypothesis. Therefore, it is worth to test if there is some thermodynamic basis for these concepts.

Figure 7 shows isothermal sections at 1273 K (1000 °C) of systems Fe-Cr-5 wt.% Ni-Mo (Fig. 7a) and Fe-Cr-5 wt.% Ni-W (Fig. 7b). In order to the Chromium equivalent expression to have some validity, the boundaries of the $\alpha + \gamma$ (BCC + FCC) field must be defined by parallel straight lines in these diagrams. In this case there is some expectancy that, for example, the volume fractions of ferrite and austenite will not be affected by the molybdenum content in the alloy as substitute for Chromium. It is observed that this is approximately the case, in particular for the Fe-Cr-Ni-Mo system, but a closer analysis of the case of system Fe-Cr-Ni-W shows that the two boundaries of the $\alpha + \gamma$ field have slightly different slopes. Parallel phase boundaries do not necessarily result in parallel phase fraction lines, since the present calculations refer to the two dimensional section of a four dimensional space, and the tie-lies of the equilibrium are not contained in this projection. The present calculations seem, however, to validate this linearity. To prove this, the isomolar fraction lines for austenite (which are obviously complementary to the isomolar fraction lines for ferrite in the two-phase field), are plotted in the quaternary and higher order isothermal sections. They are also defined, in the present case, by straight lines with approximately the same slope as the $(\alpha + \gamma)$ boundaries. Notice, however, that the isomolar fraction lines are not evenly distributed across the two-phase field, as it would happen if they were defined by the lever rule.

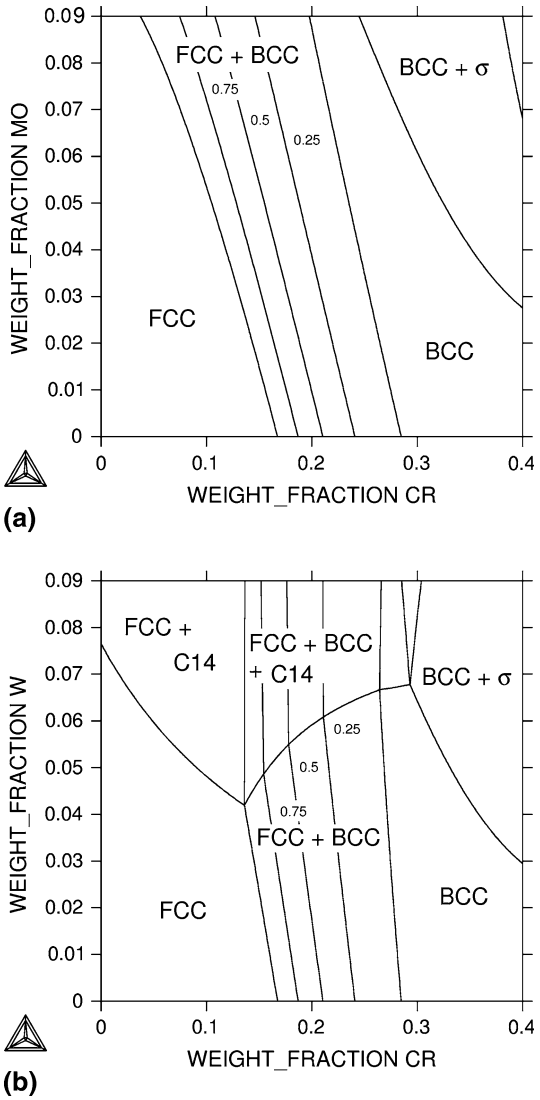

Fig. 7 Isothermal section of system (a) Fe-Cr-5 wt.% Ni-Mo and (b) Fe-Cr-5 wt.% Ni-W at 1273 K (1000 °C)

The pre-factor of Mo in the Chromium equivalent expression used in Schaeffler's diagram is unity and the results shown in Fig. 7(a) corroborates this, since the $\gamma/\alpha + \gamma$ border of the two-phase field runs from approximately ~16.75 wt.% Cr at 0.0 wt.% Mo to ~6.0 wt.% Cr at 7.8 wt.% Mo, resulting in a slope of about −1.37, the $\alpha/(\alpha + \gamma)$ boundary, on the other hand, runs from ~28.5 wt.% Cr at 0.0 wt.% Mo to ~21 wt.% Cr at 7.7 wt.% Mo, leading to a slope of −0.97, the "average" slope would be −1.17, which is indeed, close, to unity.

The inclusion of W in the present calculations is not arbitrary. Tungsten is an important alloying element in duplex steels, having beneficial effects on the pitting corrosion resistance, and yet, tungsten is not included in the Chromium equivalent expression used in Schaeffler diagram. There have been some suggestions that W should

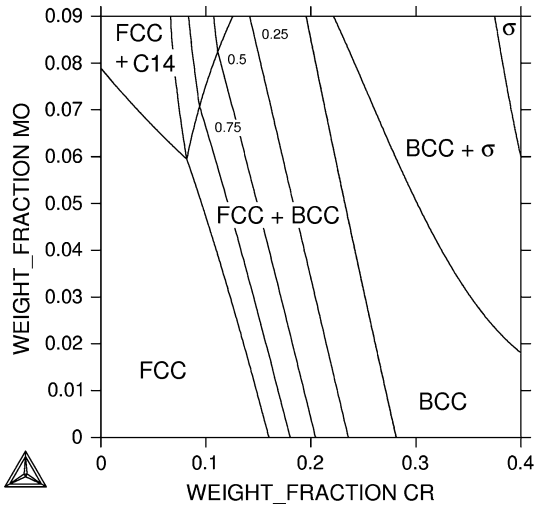

Fig. 8 Isothermal section of system Fe-Cr-5 wt.% Ni-1 wt.% W-Mo at 1273 K (1000 °C)

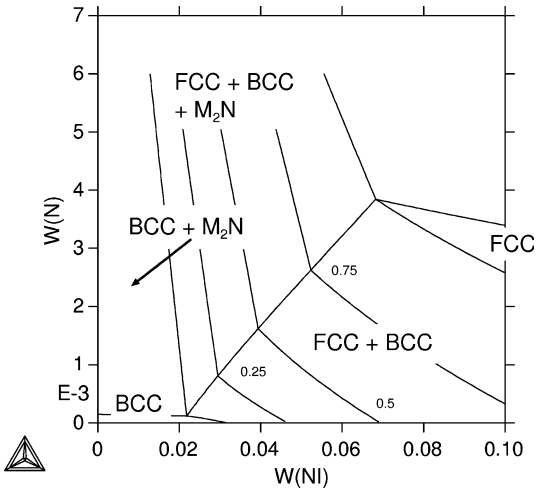

Fig. 9 Isothermal section of system Fe-25 wt.% Cr-Ni-N at 1273 K (1000 °C)

behave equivalently to Mo. The present calculations (Fig. 7b) seem to disagree with this hypothesis, since the "average" slope of the borders of the two-phase field in the Fe-Cr-Ni-W system is −0.536, therefore adopting a pre-factor of 0.5 for W would be more appropriate.

Anyway, even considering that the present calculations seem to validate the concept of Chromium equivalent, it is obvious that the parameter has limits of validity imposed by the precipitation of intermetallics, as the sigma or the Laves phases. In the case of the Fe-Cr-Ni-W system, for example, the maximum W content which can be dissolved in duplex steels without precipitating the Laves phase at 1273 K ranges from ∼4 to ∼6 wt.%. It is suggested, therefore, that applicability of the Chromium equivalent expression should be limited to some value, probably the smallest concentration in which precipitation of intermetallics can be safely prevented.

Figure 8 shows the 1273 K isothermal section of system Fe-Cr-5 wt.% Ni-1 wt.% W-Mo. Comparing with Fig. 7(a), it is observed that, indeed, the phase boundaries of the $\alpha + \gamma$ equilibria move about 0.5 wt.% Cr towards pure iron, which would corroborate the additivity predicted by the Chromium equivalent expression, however, notice that the limit concentrations to precipitate the Laves phases moved to ∼6 wt.% Mo. In Fig. 7(a) it is observed that the limit Mo concentration is larger then 9 wt.%, the addition of 1 wt.% W is enough to bring this limit to 6 wt.% Mo. This shows that some degree of synergy exists between both elements in solid solution in duplex stainless steels.

As in the case of the Chromium equivalent, Nickel equivalent is also validated by the present calculations. This is demonstrated by the isothermal section at 1273 K of system Fe-25 wt.% Cr-Ni-N (Fig. 9). The boundaries of the $\alpha + \gamma$ field (FCC + BCC) are marked approximately by parallel straight lines. Nitrogen is not traditionally included in Nickel equivalent expressions, but in some cases it is tacitly assumed that this element should have the same pre-factor as carbon (=30). Based on the slope of the lines in the present calculation an "average" slope of −51.5 is calculated, this suggests a pre-factor close to 50 and, considering the imprecision of this estimation, adopting the same pre-factor as carbon seems to be more acceptable. In any case, the maximum possible amount of nitrogen in duplex steels is limited by the precipitation of the M_2N nitride, and this depends approximately linearly on the Nickel concentration in the alloy. This is due in part to the increased austenite molar fraction as Nickel increases, as evidenced by the isomolar fraction lines for austenite, depicted in Fig. 9.

A last test of the concepts of Chromium and Nickel equivalent is shown in Fig. 10, which presents the 1273 K isothermal section of systems Fe-24 wt.% Cr-1 wt.% Mo-Ni-N (Fig. 10a) and Fe-24.5 wt.% Cr-1 wt.% W-Ni-N (Fig. 10b). According to the Chromium equivalent expression 1 wt.% Mo is equivalent to 1 wt.% Cr and following our results 1 wt.% W corresponds to 0.5 wt.% Cr, therefore these sections should be completely identical to the one shown in Fig. 10. Indeed, the phase diagram topology is identical and even the coordinates of the lines seem to be identical in the low Ni region (e.g. in the $\alpha/\alpha + \gamma$ boundary). There are, however, quantitative differences in the high Ni region, as evidenced by the $\gamma/\alpha + \gamma$ boundary, since coordinates corresponding to the maximum N content in which austenite in equilibrium with ferrite without precipitating M_2N are ∼7 wt.% Ni and ∼0.004 wt.% N in Fig. 9, ∼8.5 wt.% Ni and ∼0.003 wt.% N in Fig. 10(a) and ∼8 wt.% Ni and ∼0.0031 wt.% N in Fig. 10(b), showing that in this case the effects of Ni, Mo, W and N are not additive.

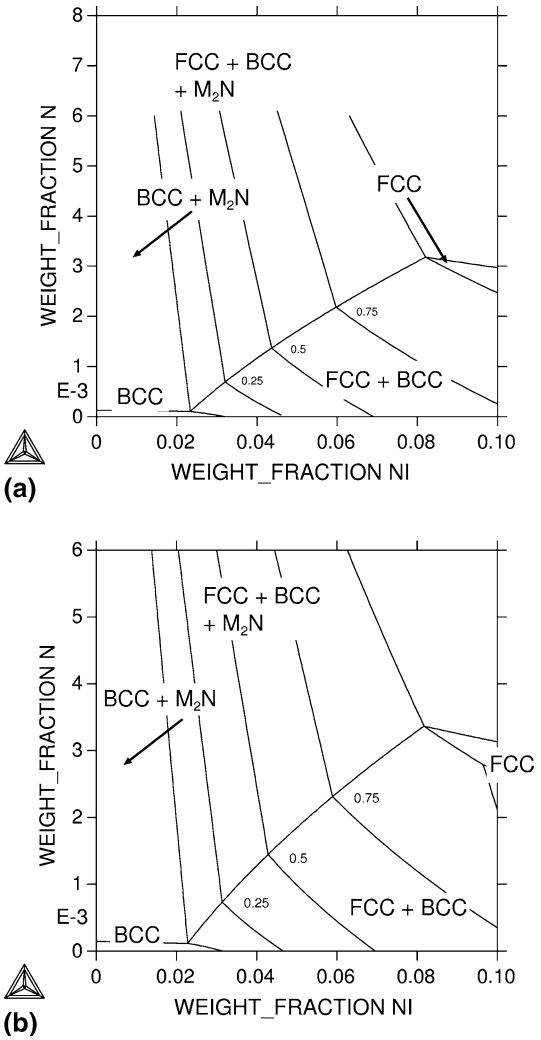

Fig. 10 Isothermal sections of systems Fe-24 wt.% Cr-1 wt.% Mo-Ni-N (a) and Fe-24.5 wt.% Cr-1 wt.% W-Ni-N (b) at 1273 K (1000 °C)

In summary, the concepts of Chromium equivalent and Nickel equivalent appear to be validated by the present calculations, provided the concentrations of the alloying elements other than Cr and Ni are not too high. Naturally, this depends on the adopted thermodynamic models, if the model does not include terms due to the interaction between Cr, Mo and W, their effect will indeed be additive in the alloy. This is not, however, the present case, since the quaternary systems shown in Fig. 7, 8, and 9 have been properly assessed based on independent experimental data.

3.3 Constitutive Diagrams for σ and M_2N Precipitation

In the metallurgy of duplex steel and, in particular, in welding technology, several problems arise which would profit from a tool like the Schaeffler diagram. Two of the most important are the susceptibility to sigma phase and M_2N precipitation. The results shown in Fig. 7 and 9 suggest, however, that intermetallic precipitation is a non linear process and it is unlikely that a simple linear tool as the Schaeffler diagram would be capable to handle this complexity. In Fig. 4 the field of sigma phase is delimited by a curve with a complex shape, confirming this complexity.

The same could be said of the precipitation of the M_2N nitride, the key factors seems to be the nitrogen content of the alloy and the amount of austenite in the microstructure, but complex interactions between the alloy components are possible.

The situation is more complex because a proper thermodynamic calculation is able to provide a precise answer to these questions without the need to use phenomenological tools; after all, as defended in this work, the existing databases are reliable for modeling duplex steels. Therefore, although the present results allow to validate Schaeffler diagram as a tool to predict the basic microstructure of austenitic stainless steels, particularly in duplex stainless steels, computational thermodynamics should be used for more complex problems, like the susceptibility the alloy presents for intermetallics or nitride precipitation.

4 Conclusions

Although the Schaeffler diagram, and similar ones, started as empirical technological tools, the present calculations showed they are based on in thermodynamic equilibria at some key temperatures that are process related. Their usefulness is, therefore validated.

The concept of Chromium and Nickel equivalents is fundamental for the usefulness of these tools. The present calculations suggest that they represent valid equilibrium relations in the multicomponent stainless steels and, provided the concentrations for the elements other than Cr and Ni are kept limited, they should reflect approximately the phase relations in these alloys.

In the cases studied in the present work: molybdenum, tungsten and nitrogen. The present calculations validate the pre-factor of Mo in the Chromium equivalent expression. A pre-factor of 0.5 is suggested for W and, although the calculations suggest a higher value, adopting the same pre-factor as carbon (30) for nitrogen is recommended. The Schaeffler diagram, as well as similar tools, are technological tools, and hence, emphasis is on ease of application, and not on precision.

Concerning the precipitation of intermetallic phases, like sigma or Laves, and/or of Chromium nitrides, known problems of welding metallurgy of stainless steels, the present results suggest that it is unlikely that a similar technological tool, as the Schaeffler diagram, could be

devised, since this type of problem is markedly non-linear. Therefore, it is recommended that proper thermodynamic calculations be performed whenever this kind of problem is targeted, instead of using simplified tools.

Acknowledgments The authors would like to thank Eng. Caio de Paula Camargo Pisano (Aperam South America, São Paulo, Brazil) for useful discussion concerning milling of duplex stainless steels. The present work was supported by the Brazilian National Research, Innovation and Development Council (CNPq, Brasília, Brazil) under Project 312424/2013-2, and by the Fundação de Amparo à Pesquisa do Estado de São Paulo (São Paulo, Brazil) under Project 2016/05768-2. This support is gratefully acknowledged.

References

1. A.L. Schaeffler, Selection of Austenitic Electrodes for Welding Dissimilar Metals, *Weld. J.*, 1947, **26**(10), p 1-20
2. A.L. Schaeffler, Welding Dissimilar Metals with Stainless Electrodes, *Iron Age*, 1948, **162**, p 72-79
3. A.L. Schaeffler, Constitution Diagram for Stainless Steel Weld Metal, *Metal Prog.*, 1949, **56**(11), p 680
4. W.T. DeLong and H.F. Reid, Jr., Properties of Austenitic Chromium in Austenitic Chromium-Manganese Stainless Steel Weld Metal, *Weld. J.*, 1957, **37**(1), p 1-8
5. C.J. Long and W.T. DeLong, The Ferrite Content of Austenitic Stainless Steel Weld Metal, *Weld. J.*, 1973, **52**(7), p 281s-297s
6. T.A. Siewert, C.N. McCowan, and D.L. Olson, Ferrite Number Prediction to 100 FN in Stainless Steel Weld Metal, *Weld. J.*, 1988, **67**(12), p 289-s-298-s
7. D.J. Kotecki and T.A. Siewert, WRC-1992 Constitution Diagram for Stainless Steel Weld Metals: A Modification of the WRC-1988 Diagram, 1992, *Weld. J.*, 1992, **71**(5), p 171s-178s
8. D.L. Olson, Prediction of Austenitic Weld Metal Microstructure and Properties, *Weld. J.*, 1985, **64**(10), p 281s-295s
9. R.D. Thomas, Jr., A Constitution Diagram Application to Stainless Weld Metal, *Schweizer Archiv fur Angewandte Wissenschaft und Technik*, 1949, **1**, p 3-24
10. E. Yamamoto, K. Shiga, R. Kayano, T. Okazaki, H. Watanabe, T. Kiso, T. Tahara, and F. Minami, Guidelines for Repair Welding of Pressure Equipment in Refineries and Chemical Plants, *J. Press. Vessel Technol.*, 2013, **135**(3), p 034501-034501-12. doi:10.1115/1.4023729
11. K. Frisk, A Thermodynamic Evaluation of the Cr-Fe-N System, *Metall. Mater. Trans. A*, 1990, **21**(9), p 2477-2488
12. A.V. Khvan, B. Hallstedt, and C. Broeckmann, A Thermodynamic Evaluation of the Fe-Cr-C System, *CALPHAD*, 2014, **46**, p 24-33